Available online at www.sciencedirect.com
SCIENCE DIRECT®
Applied Catalysis A: General 267 (2004) 251–265
APPLIED CATALYSIS A: GENERAL
www.elsevier.com/locate/apcata

New effects during steam gasification of naphthalene: the synergy between CaO and MgO during the catalytic reaction

Nelson Alarcón [d], Ximena García [a,*], Miguel Angel Centeno [c], Patricio Ruiz [b], Alfredo Gordon [a]

[a] *Departamento de Ingeniería Química, Universidad de Concepción, Chile*
[b] *Unité de Catalyse et Chimie des Matériaux Divisés, Université Catholique de Louvain, Belgium*
[c] *Departamento de Química Inorgánica e Instituto de Ciencia de Materiales de Sevilla, Universidad de Sevilla-CSIC, Sevilla, Spain*
[d] *Escuela de Ciencias Ambientales, Universidad Católica de Temuco, Chile*

Received in revised form 24 February 2004; accepted 6 March 2004

Available online 15 April 2004

Abstract

The catalytic activity of commercial CaO and MgO and their physical mixtures on the gasification reactions with steam was studied.

Steam gasification of naphthalene as model reaction was selected and experiments in a laboratory scale reactor were performed. Carbon conversion for pure MgO and CaO was 54 and 62%, respectively. Every mixture showed a larger conversion than the weighted average of the pure compounds conversions; i.e., they exhibited catalytic synergy. The largest catalytic activity, reflected by the carbon conversion (79%), was obtained with a 10% CaO + 90% MgO mixture, which also showed the highest catalytic synergy (44.2%) among the assayed mixtures.

Characterization of catalysts by XPS, XRD, SBET and DTG/DTA lead to conclude that formation of new phases, sintering, modification of dehydration or carbonation of the oxides in the mixture could not explain synergy, or basicity changes. Oxides forming the mixture have not been modified by the preparation or during the catalytic gasification. A catalytic cooperation between the two separated oxides is observed. Thus, synergy is attributed to MgO presence in the mixture, which inhibits formation of carbonaceous material as well as bidentate carbonate in the CaO surface, while promotes the formation of unidentate carbonate of lesser stability at the reaction temperature and in the presence of $H_2O_{(v)}$.

Keywords: Catalytic gasification; Model compound; Calcium oxide; Magnesium oxide

1. Introduction

Gasification of solid fuels such as coal, biomass and solid organic wastes converts them into higher energy value gaseous products (mainly H_2 and CO), thus facilitating a more effective and cleaner use of those energy-valuable organic materials. However, gasification generates considerable amounts of condensable (tars). These mainly aromatic byproducts are ascribed as responsible for operational problems, such us fouling and clogging of pipes and equipments. Furthermore, these tars possess mutagenic characteristics and pollute industrial waters. A technological alternative is to perform the catalytic reaction with steam as gasifying agent by using CaO or MgO as catalysts. García [1] confirmed the thermodynamic feasibility of steam gasification, at conditions in which CaO acts as a catalyst for that reaction. In fact, high temperatures favor the formation of hydrogen and carbon monoxide as the main reaction products for steam gasification of naphthalene, a model reaction for tar gasification. Therefore, this catalytic process can contribute not only to reduce the formation of tars, but also to enhance the yield and the calorific value of the resulting gas. Additional advantages of CaO and MgO as gasification catalysts are their low cost and widespread availability.

The catalytic activity of CaO and MgO has been tested using naphthalene as a model compound for gasification [1–4], due to its high thermal stability and large concentration in those tars formed during coal gasification. García and Hüttinger [2] described gasification as a sequential two-step process: (i) thermal decomposition (pyrolysis) of naphthalene to gaseous products and solid carbon deposition on the catalyst's surface (CaO obtained by limestone calcination);

* Corresponding author. Tel.: +56-41-204534; fax: +56-41-247491.
E-mail address: xgarcia@diq.udec.cl (X. García).

0926-860X/$ – see front matter © 2004 Elsevier B.V. All rights reserved.
doi:10.1016/j.apcata.2004.03.010

(ii) gasification with steam of the deposited carbon. These authors reported a good catalytic activity exhibited by CaO, and proposed a Langmuir–Hinshelwood-type kinetic model that satisfactorily described the experimental results. Betancur et al. [3] extended that study to the utilization of MgO and dolomite ($MgO \cdot CaO$) as catalysts, assaying the effect of operation variables on the catalytic activity of the different oxides as well as the possible inhibitory effect of sulfur in the reactive atmosphere. Results showed that sulfur does affect the catalytic activity of CaO and MgO but does not completely poison them, which constitutes an advantage over more traditional nickel-based catalysts. That work also showed that the catalytic activity of the oxides decreases in the following order: MgO > dolomite ($MgO \cdot CaO$) > limestone (CaO). The gasification of real tars at laboratory scale utilizing the developed CaO catalyst showed promising results [4].

In general, literature shows that, alkaline earth oxides present significant catalytic activity and selectivity in the gasification of tars to gaseous products. The principal difficulty found among these oxides is related to catalyst deactivation by carbon deposition and carbonate formation. CaO seems to be more active than MgO but much more prone to deactivation, particularly by carbonate formation [2]. On the other hand, experiments with MgO have shown no deactivating effects either by carbonate formation, or by carbon deposition. Other preliminary assays showed an interesting result [5], as a significant increase in the production of gaseous products (mainly CO and H_2) was observed upon mixing MgO with CaO. Important is the fact that, although the catalyst contained CaO, it was not deactivated during the reaction and the mixture activity remained constant during a long lasting experiment.

Further and more detailed results are given in this work, concerning the catalytic performances of pure CaO, pure MgO and their physical mixtures for naphthalene's gasification. Our objective is to compare the catalytic activity of the pure oxides with that of their mixtures. To discern on the influence of the catalyst components during gasification, the effect of the mixture composition was evaluated and several analytical techniques were used to get a comprehensive characterization of the bulk and the surface of catalysts, before and after the reaction. The characterization included the following techniques: (i) BET area determination to follow the evolution of the specific surface area; (ii) XRD analyses to study the formation of new phases during the catalysts pretreatment or the catalytic reaction, and the stability of the crystallographic phases during reaction; (iii) TGA analyses, for basicity determination in solids exposed to CO_2 adsorption; (iv) DTG/DTA analyses to determine evolution of the solids as a function of temperature, in order to find out hydration and carbonation states of the catalysts.

The surface characterization of the catalysts has been complemented with DRIFTS and XPS analyses. These results have been presented extensively in a previous work [5]. In the present paper, only the essential points of these results are included with the aim to complete the characterization of the catalysts and to support the discussion. In particular, DRIFT (in situ) experiments were performed to determine the basicity of catalysts by chloroform adsorption and after pretreatment of the samples with CO_2 and/or steam at reaction temperature, to simulate gasification conditions. XPS was selected for identification of surface atoms, carbon and carbonate formation, transfer of the atoms in surface (mutual contamination of the oxides) and for the determination of the carbon and oxygen forms on the surface.

2. Experimental

2.1. Catalyst preparation

CaO (Riedel de Häen, 96% purity) and MgO (BDH Chem., light, 95% purity) were selected as catalyst precursors. Mixing 100 g of the dried oxides for 20 min and then adding distillated water until a mud was obtained produced physical mixtures of the required weight composition of the two oxides. Afterwards the wet mixture was submitted to drying at room conditions for approximately 100 h and, finally, at 378 K in an oven. The calcium oxide content in the CaO/MgO mixtures was 5, 10, 30, 50, 70 and 90 wt.%. Calcination of the catalysts, pure oxides and mixtures, was carried out "in situ", i.e. within the gasification reactor by heating up to reaction temperature, in argon (99.999% pure) atmosphere, for 30 min.

2.2. Pretreatment of catalysts

The catalyst samples were subjected to the reaction temperature (1033 K) for 2 h, either in argon, or in the case of pure CaO, pure MgO and the 10% CaO + 90% MgO mixture sample, in a steam atmosphere as well.

2.3. Catalytic test

Catalytic activity was measured during steam gasification of naphthalene, as model compound. The experimental runs were carried out in a stainless steel fixed bed laboratory reactor (length = 40 mm, internal diameter = 30 mm) described elsewhere [2]. The naphthalene-steam molar ratio of the feed was kept at 1/20, enough to assure complete gasification of naphthalene. The gas flow was varied to achieve residence times (calculated as the ratio between effective reaction volume and volumetric flow at the reaction temperature) in the range of 0.5–10 s. The gaseous products (H_2, CO, CO_2 and CH_4) were analyzed by on-line gas chromatography using a Perkin-Elmer, 8700 GC, and a Porapaq Q column. In all tests (pure oxides and their mixtures), 15 g of catalyst were loaded to the reactor with particle size: 1–2 mm, which formed a 4 cm height catalytic bed. At the selected operating conditions, absence of diffusion limitations has been previously demonstrated [1]. Further details of the equipment and

experimental procedure are presented elsewhere [1–4]. Some experimental runs with an inert bed of ceramic material were utilized for comparison and as a controlling assay.

Carbon conversion, defined as the fraction of elemental carbon of the naphthalene molecule converted to the C-containing gaseous CO, CO_2 and CH_4 is calculated as follows:

$$X_C = \frac{\dot{n}_{CH_4} + \dot{n}_{CO} + \dot{n}_{CO_2}}{10 \times \dot{n}_{o,N}} \quad (1)$$

In Eq. (1), $\dot{n}_i$ represents molar flow of products ($i = CH_4$, CO, CO_2), and $\dot{n}_{o,N}$ is the molar flow of naphthalene fed to the reactor.

Product yield is determined as

$$Y_i = \frac{\dot{n}_i}{\dot{n}_{oN}} \left(\frac{\text{mole}_i}{\text{mole}_{\text{naphthalene}}} \right) \quad (2)$$

The deviation in the value of conversion of the CaO + MgO mixture from the expected weighted average conversion calculated from the pure oxides was quantified as a percentage of synergy, defined by

$$\%\,\text{synergy} = \frac{X_{C,\text{mixture}} - (X_{C,CaO} \cdot \%CaO + X_{C,MgO} \cdot \%MgO)}{X_{C,CaO} \cdot \%CaO + X_{C,MgO} \cdot \%MgO} \times 100 \quad (3)$$

2.4. Catalysts characterization

Fresh and used samples were characterized by the following techniques.

2.4.1. BET areas

BET surface areas of the samples were determined by the one point method using adsorbed nitrogen at 77 K, in a Micromeritics Flowsorb II 2300 instrument. The solids were previously degassed at 423 K for 2 h under gas flow (30% N_2, 99.9995% and 70% He, 99.9995%). The surfaces areas of the fresh solids calcined at 473 K, in air at the reaction temperature were also measured.

2.4.2. X-ray diffraction

XRD analysis was carried out with a Kristalloflex difractometer Siemens D5000, equipped with a copper anode (Cu Kα; λ = 1.5418 Å). The equipment's operational conditions were 40 kV, 50 mA. The 2θ range between 5° and 80° was scanned at a rate of 0.2°/min. Identification of the crystalline phases was carried out by using JCPDS database [6].

2.4.3. TGA analysis

The thermal desorption of CO_2, previously adsorbed for 60 min at 323 K was considered. N_2 (99.998%) was used as carrier gas and the temperature was raised to 1073 K at a heating rate of 5 K/min. Volumetric flows of CO_2 and N_2 were kept constant at 150 ml (STP)/min. A thermogravimetric balance (Cahn 2000, model 113X), equipped with a temperature programmer controller (Micricon 823), a vacuum system and a flow measuring-controller (Brooks), was used to carry out these measurements.

2.4.4. DTG/DTA analysis

A thermo analyzer (Setaram-TGA 92), equipped with a microbalance (B 92), an oven reaching up to 2023 K and a PC-linked controller for the oven temperature and the gas flows at the entrance and exit, was used. Calcination of the solids and combustion of deposited char were performed in a He/O_2 atmosphere (30 ml He + 30 ml O_2). A sample of approximately 25 mg was placed in a 10 μl alumina pan, and the temperature was raised from ambient to 1073 K, at 5 K/min.

2.4.5. DRIFT analysis

A FTIR spectrometer Brucker IFS 88, with KBr optics and a DTGS detector, in the 4000–400 cm^{-1} range, was used. The spectral resolution was 4 cm^{-1}. The signal/noise ratio was maximized for accumulation of 200 scans and the reference spectrum was obtained from an aluminum mirror, thus allowing automatic spectra correction by subtraction. An atmosphere and temperature controlled chamber (Spectra-Tech 0030-103), with ZnSe windows, was used. The samples were placed without any treatment, such as pressure or dilution, inside the environment-controlled chamber.

For basicity determinations, FTIR spectra before and after $CDCl_3$ adsorption were analyzed [5]. Software (Brucker OPUS/IR 2.2) was used to calculate band intensities after correction of the base line by a polynomial function. The samples (particle size <0.2 mm) were placed in the analysis chamber, heated up to 1033 K and pretreated for 2 h with N_2 (30 ml/min), before adsorption. The out-gassed sample was subjected to $CDCl_3$ adsorption for 30 min. The DRIFT spectra were registered on the fresh sample and before and after adsorption. The areas of the adsorbed $CDCl_3$ bands were calculated with the above-indicated software.

Fresh catalysts were analyzed after treatment under a CO_2 and steam atmosphere at 1033 K (the reaction temperature). After out-gassing the samples at 1033 K for 60 min. under N_2 flow (30 ml/min), CO_2 desorption was monitored. They were cooled to room temperature and subjected to a CO_2 flow for 15 min after which each sample was heated sequentially, again under N_2 flow (30 ml/min) up to 423, 573, 723, 873 and 1033 K, kept for 30 min at each temperature and a spectrum was recorded at each listed temperature. At 1033 K, the exposure to CO_2 flow was followed by treatment under wet nitrogen (obtained by bubbling N_2 in liquid water at room temperature) and the corresponding DRIFT spectrum was recorded. More details about the above experiments are given elsewhere [5].

2.4.6. XPS analysis

Surface composition, deposited carbon and variations of binding energies of the C 1s, O 1s, Mg 2s and Ca 2s

peaks of selected samples were obtained by XPS analysis. Pressed samples, protected from charge effects, were out-gassed overnight at 7×10^{-7} mbar vacuum and room temperature. The X-ray photoelectron spectroscopy data were obtained with a Surface Science Instruments SSX-100 model 206 spectrometer with a monochromatic Al Kα source, operating at 10 kV and 20 mA. The residual pressure inside the analysis chamber was below 6.7×10^{-7} Pa. For analysis, the C 1s peak (of deposited C) was used as reference by adjusting its binding energy C–(C–H) to 284.8 eV; peak decomposition was performed with a Gaussian/Lorentzian ratio of 85/15. Atomic compositions were calculated by using the Schofield's sensitivity factors after normalization of the peak's areas, allowing calculation of relative atomic concentration ratios for comparison among samples [5].

3. Results

3.1. Catalytic activity

Fig. 1a–d show gas yield and carbon conversion, respectively, as function of the residence time, using MgO, CaO and a mixture 10% CaO + 90% MgO as gasification catalysts. For all catalysts, H_2 was the main gaseous product, followed by CO, CO_2 and CH_4. No other component in the gas phase was detected. Carbon conversion increases with residence time leading to final conversions lower than 1.0 in the range of working residence times. Similar results were observed for the other mixtures.

Fig. 2a shows catalytic activity (expressed as carbon conversion) of CaO/MgO mixtures, as a function of the mixture composition; shown values were determined at 1033 K and 4 s of residence time in the reactor. A synergetic effect in the catalytic activity is observed for the CaO/MgO mixtures. Catalytic activity of all prepared mixtures showed to be higher than that exhibited by either of the pure oxides, CaO or MgO, resulting the 10% CaO + 90% MgO mixture the most active, with a 44.2% synergy, as calculated from Eq. (3). Other residence times were assayed as well and in all cases the synergetic effect was verified.

H_2 production is not considered in the calculation of carbon conversion (see Eq. (1)) but Fig. 2b shows that H_2 yield varies, like the carbon conversion, with the mixture composition and the same synergetic effect was observed. On the other hand, Fig. 3c shows that synergy was also observed for the CO yield while the CO_2 yield remains constant.

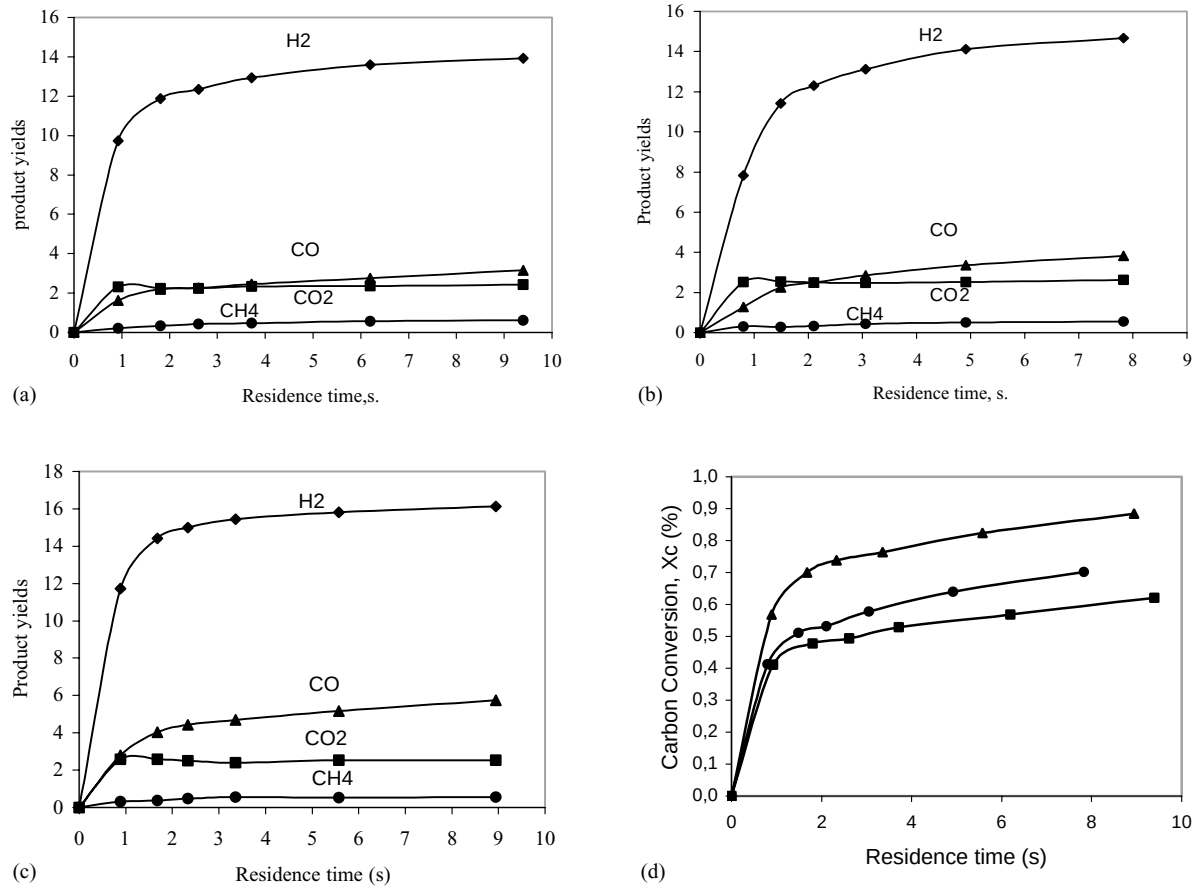

Fig. 1. Gas yields and carbon conversion at 1033 K: (a) MgO; (b) CaO; (c) 10% CaO + 90% MgO; (d) carbon conversion. Catalysts: (■) MgO; (●) CaO; (▲) 10% CaO + 90% MgO.

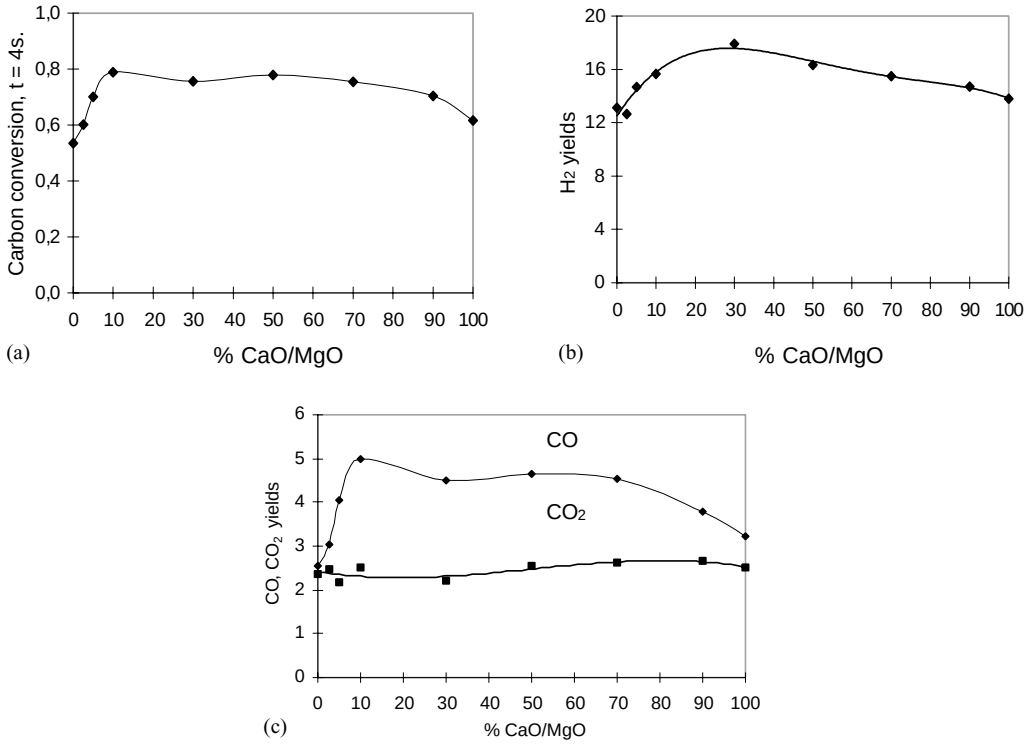

Fig. 2. (a) Carbon conversion as a function of CaO + MgO catalyst composition; (b) H_2 yields as a function of catalyst composition; (c) CO, CO_2 yields as a function of catalyst composition.

3.2. Characterization

3.2.1. BET surface area

Table 1 compares values of BET surface area for fresh (before and after calcination) and used catalysts. Additionally, the table includes BET surface area values for some samples pretreated with steam. Calcination enhances surface areas of all selected samples with the exception of 100% MgO where a slight area reduction is observed. For the fresh and calcined mixtures, the determined values of BET surface areas are similar to the values calculated as a weighted average from the pure compounds. In particular, for the 10% CaO + 90% MgO mixture the expected average value is 50.2 m^2/g while the measured value, was 51 m^2/g. On the other hand, the BET surface area for the mixture after the catalytic test was 37.1 m^2/g, a value close to the weighted average of the used pure oxide catalysts (41.6 m^2/g). During reaction, all solids lose surface area, probably due to sintering occurring by the exposure of the catalysts to the reactive atmosphere. The sintering effect of H_2O is clearly demonstrated by comparing the BET surface area of the 10% CaO + 90% MgO calcined sample with the corresponding steam-pretreated sample (51 versus 26 m^2/g). Apparently, no correlation is observed between BET surface areas

Table 1
BET surface area for CaO + MgO catalysts

Catalyst	BET area (m^2/g)			
	Fresh	Calcined	Used	$H_2O_{(V)}$-pretreated
100% MgO	69.0	53.6	44.7	32.4
2.5% CaO + 97.5% MgO	–	73.8	–	–
5% CaO + 95% MgO	–	65.5	–	–
10% CaO + 90% MgO	35.6	51.0 (50.2)	37.1 (41.6)	26.0 (30.5)
30% CaO + 70% MgO	30.9	40.6 (43.5)	32.0 (35.3)	–
50% CaO + 50% MgO	23.9	28.9 (36.7)	26.5 (29.0)	–
70% CaO + 30% MgO	19.4	25.6 (30.0)	19.2 (22.7)	–
90% CaO + 10% MgO	16.1	21.7	15.1	–
100% CaO	16.4	19.8	13.3	13.2

The values in parentheses is the expected weighted average.

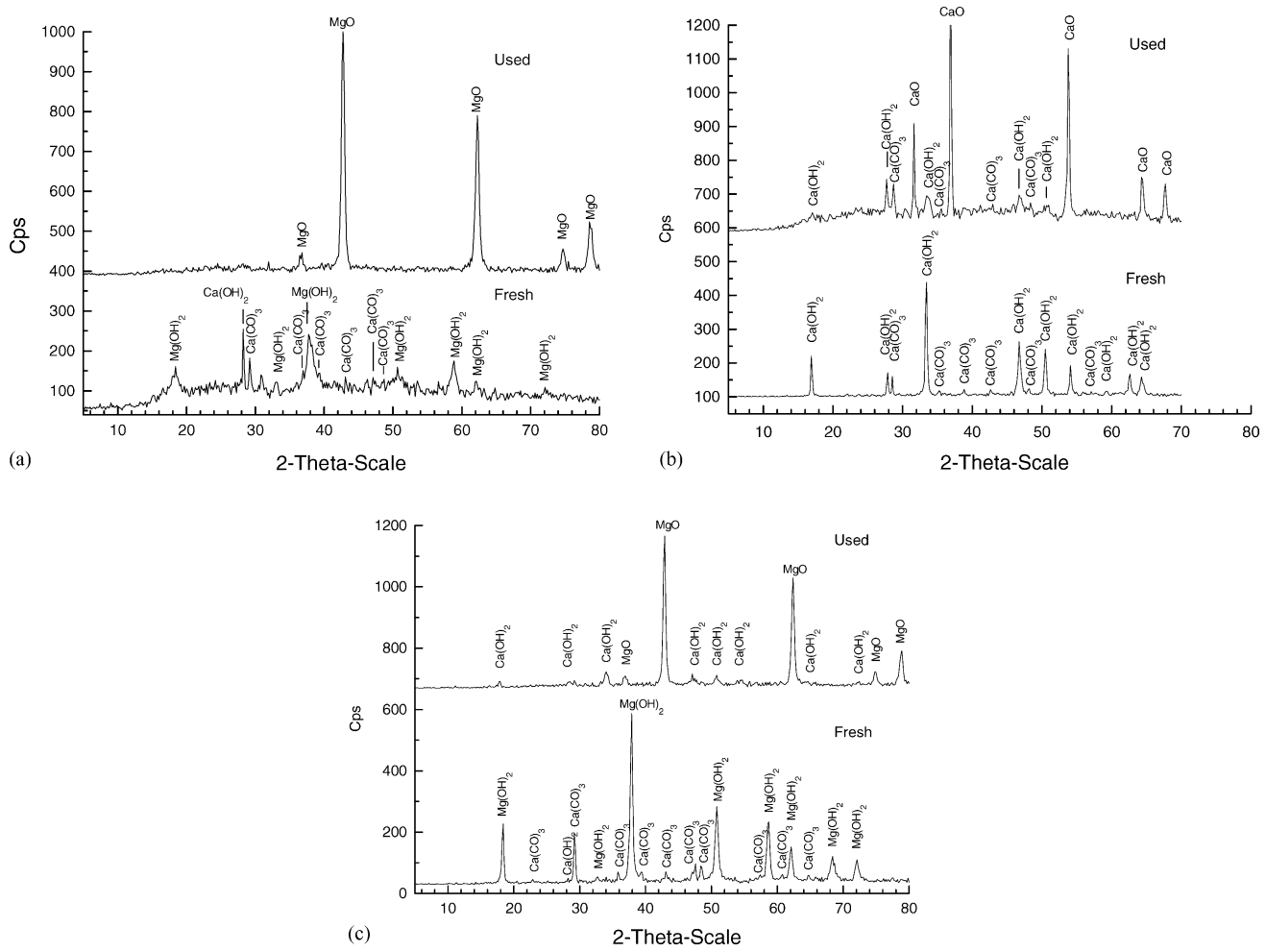

Fig. 3. XRD of selected catalysts: (a) MgO; (b) CaO; (c) 10% CaO + 90% MgO catalyst.

of the selected samples and their catalytic activity during naphthalene gasification.

3.2.2. XRD analyses

The XRD analyses of MgO, CaO and of the 10% CaO + 90% MgO mixture are shown in Fig. 3a–c. XRD-curves for fresh (calcined) and used catalyst are also presented. Hydroxides ($Mg(OH)_2$-brucite, file JCPDS, 7-0239; $Ca(OH)_2$-portlandite, file JCPDS, 4-0733) [6], formed during preparation of the catalyst, are the main phases present in the three fresh samples. In the calcium containing samples, some hydroxide phases are still present even after calcination (results not shown here) [5]. $Mg(OH)_2$-brucite was not detected after calcination of pure MgO.

For the used catalysts, hydroxides are detected in all calcium containing samples, confirming the high tendency to hydroxylation of calcium to $Ca(OH)_2$-portlandite. During gasification, hydroxides are formed by reaction of the solids with steam present in the atmosphere.

Calcite ($Ca(CO)_3$, file JCPDS: 5-0586) [6] is also detected in the calcium containing samples, which is still present in the used sample of pure CaO. Some calcite is also observed in pure MgO fresh sample; this could indicate the presence of calcium as an impurity in the MgO sample.

According to JCPDS database [6], the oxide phases found in the used catalysts (Fig. 3a–c), were MgO periclase (JCPDS file: 4-0829) and CaO lime (JCPDS file: 4-777). No other phase was detected in the mixtures of CaO + MgO; in other words, the phases present in the mixtures correspond to the contributions of the pure components.

3.2.3. TGA analysis

The amount of CO_2 adsorbed on the samples, expressed as mmol CO_2/m^2 of catalyst, and measured by TGA analysis, is presented in Fig. 4 as a function of the mixture composition. As shown, CO_2 adsorption increases with calcium content in the catalytic mixture. It may be observed that no adsorption occurs for the pure MgO while it increases sharply for mixtures with calcium contents higher than 50 wt.%.

3.2.4. DTG/DTA analysis

Table 2 and Fig. 5 show DTG/DTA results obtained for fresh and used MgO, CaO and the 10% CaO + 90% MgO mixture. The two detected DTG peaks for the fresh solids

Table 2
DTG/DTA analyses of fresh and used catalysts

Catalyst	T(K)	Fresh sample		Used sample			
		Endothermic peak		Exo-peak		Endo-peak	
		T(K)	Change	T(K)	wt.%	T(K)	wt.%
MgO	293–1073	650	33.3	773	14.6	–	–
		924	3.4				
10% CaO + 90% MgO	293–1073	646	25.9	684	–	973	8.4
		967	8.8	768	6.0		
CaO	293–1073	758	9.6	693	0.3	967	11.3
		968	8.9				

(Fig. 5a, c and e), can be attributed to dehydration and decarbonation. The fresh solids, and especially calcium, are mainly in the form of hydroxides and carbonates, which during heating in the thermo gravimetric apparatus decompose releasing H_2O and CO_2.

For the pure MgO and 10% CaO + 90% MgO samples, the first decomposition peaks appear at similar temperatures (650 and 646 K) which are lower than the temperature of the first peak for the CaO (758 K). This result indicates a beneficial effect of MgO in the mixture as it promotes decarbonation and dehydration at lower temperatures. However, this behavior changes as shown by the DTG peaks detected at higher temperatures (the second peak). For the pure CaO and the 10% CaO + 90% MgO catalysts, the peaks appear at a similar temperature, which is slightly higher than the corresponding temperature of the pure MgO sample (967/968 versus 924 K). These results show that the mixture behavior resembles that of MgO at low temperatures but that of CaO at high temperatures.

Quantification of contributions is difficult because of the different degree of carbonation that each catalyst could achieve by exposure to the ambient during preparation. However, if the peaks detected at the higher temperatures are attributed to carbonate elimination only, then it may be concluded that both, thermal stability and the amount of carbonates in pure MgO, are lower than those exhibited by the mixtures and on pure CaO.

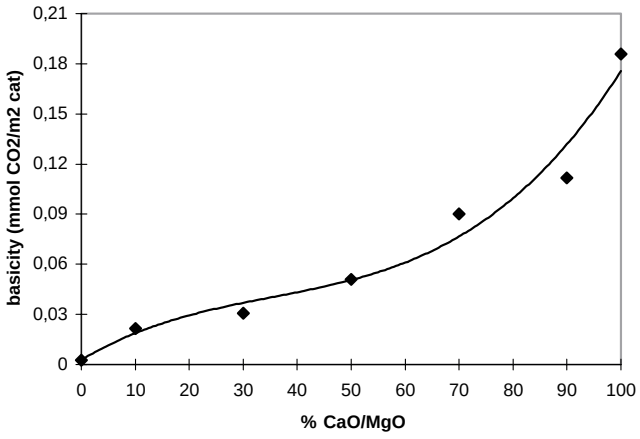

Fig. 4. Basicity after CO_2 adsorption (TGA analysis).

For the used catalysts, two DTG/DTA peaks are also identified (Fig. 5b, d and f). The first peak is attributed to combustion of the carbonaceous matter deposited on the solid surfaces; a mass diminution related to heat release (positive peak) confirms these phenomena. The second peak represents the carbonate release and it is associated to a mass loss together with heat consumption (negative peak). Only the first peak is detected for the used MgO catalyst, meaning that there are no species present in this solid that may be released at a higher temperature.

Temperatures at which carbonaceous matter combustion occurs increase in the order CaO < 10% CaO+90% MgO < MgO. This result suggests that the combustion of the deposited carbonaceous material is better catalyzed by CaO than by MgO. However, in the absence of a better char characterization it is not possible to assure that this effect is due to the effect of the solid, or it is due to differences in the carbonaceous material deposited on the solids. Table 2 and Fig. 5 show that the pure oxides present a sole exothermic event, produced by the combustion of the carbonaceous material (773 and 693 K, for MgO and CaO, respectively). By contrast, the mixture exhibits two exothermic events, one at 684 K, which is close to the value exhibited by pure CaO (693 K), and a second at 768 K, which is close to the event exhibited by pure MgO (773 K). Thus, it can be inferred that the combustion of the carbonaceous material in the mixture takes place as if this material were deposited independently on CaO and MgO, each component contributing to a characteristic and well-defined exothermic event.

A re-adsorption of the CO_2 produced during the combustion of carbonaceous material is observed in the CaO and in the mixture, but not in the MgO. The weight increase corresponding to this CO_2 re-adsorption have been pointed in the TG curves of Figs. 5d and f, at approximately 725 K for the CaO and 660 K for the 10% CaO + 90% MgO mixture.

3.3. DRIFTS analysis

3.3.1. Basicity determination

DRIFT spectra (Fig. 6) of adsorbed $CDCl_3$ in fresh solids (MgO, CaO and 10% CaO + 90% MgO) showed two adsorption peaks for $CDCl_3$, corresponding to weak and strong basicity thus allowing the determination of the

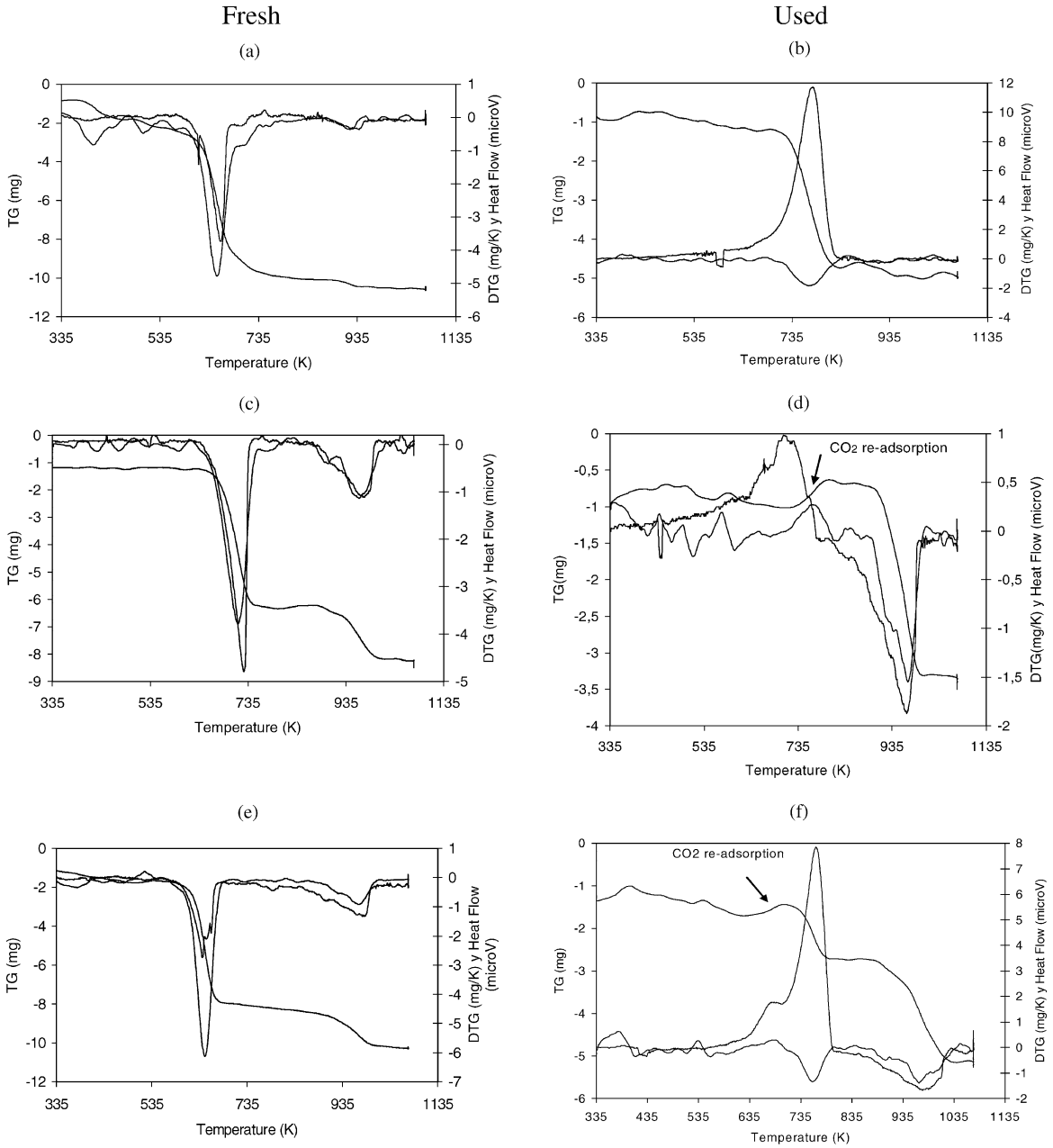

Fig. 5. DTG/DTA spectra of fresh and used catalysts: ((a) and (b)) MgO; ((c) and (d)) CaO; ((e) and (f)) 10% CaO + 90% MgO.

amount of strong and weak basic sites. The strong basicity values for CaO, MgO and 10% CaO + 90% MgO were 42.53, 11.7 and 11.42 absorbance units (a.u), respectively, which are significantly higher than weak basicity of 0.60, 0.42 and 0 for the same catalysts [5]. Basicity of CaO is higher than MgO, but these values do not correlate with their tested catalytic activity. Thus, basicity plays a role but it is not unique with regard to the activity of the assayed catalysts.

3.3.2. Reactive atmosphere simulation

On the other hand (Fig. 7), the fresh solids were subjected to CO_2 adsorption at ambient temperature, later to decarbonation by a temperature increase and to a second treatment by exposing them to CO_2 and $H_2O_{(V)}$, as observed in curves 8–10 of Fig. 7. Extended details of these results were presented elsewhere [5], so here we summarize those results that are relevant to the carbonation problem stated above. DRIFT spectra of the fresh and treated samples showed peaks representative of unidentate carbonates, hydroxyls and adsorbed water in all fresh samples. After exposure to CO_2 at room temperature, the solids are carbonated and hydrated, as expected. Subsequent heating of the samples eliminates adsorbed water and, at the same time, an OH band at 3700 cm^{-1} appears. After degasification at 1033 K hydroxides are still present only in the 100% MgO

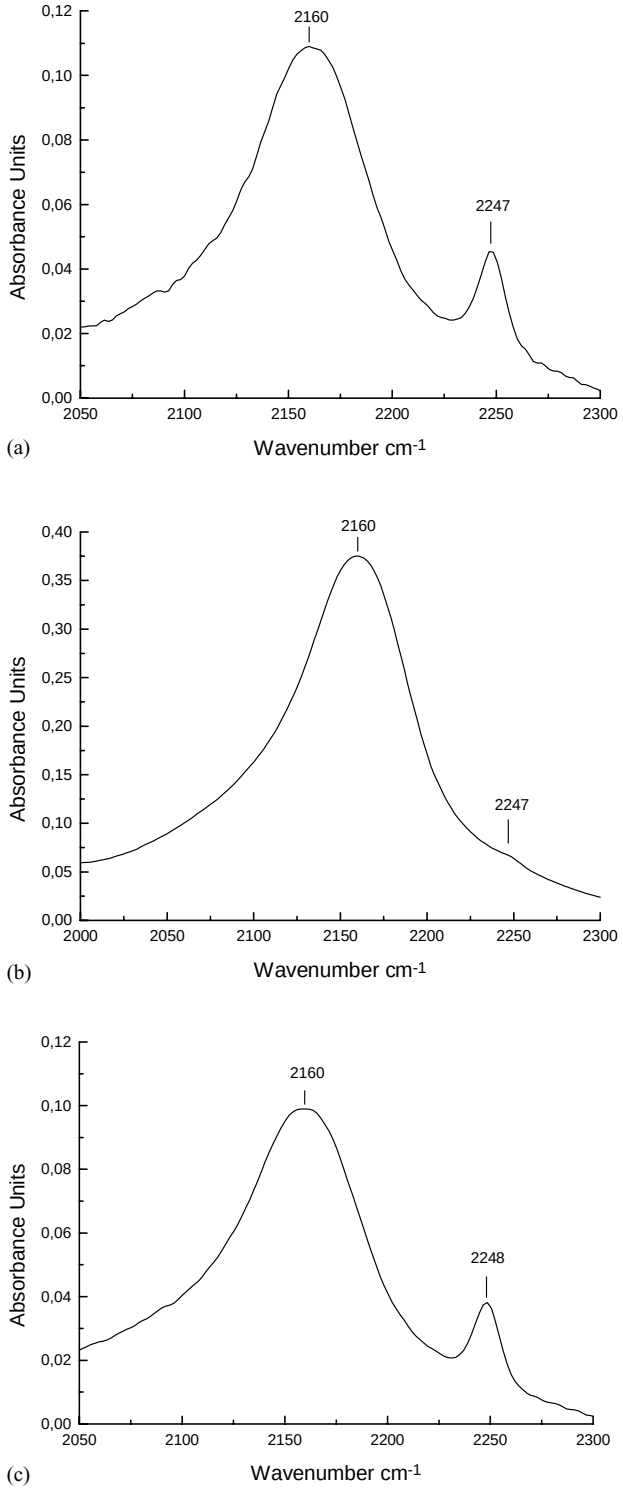

Fig. 6. DRIFT spectra of adsorbed $CDCl_3$, in fresh catalysts treated "in situ" at 1033 K: (a) MgO; (b) CaO; (c) 10% CaO + 90% MgO.

and the mixture, while carbonates remain only on the calcium containing samples, as shown by curve 7 in Fig. 7.

As the temperature rises, unidentate carbonate decreases in pure MgO and in the mixture due to CO_2 release. On the contrary, in pure CaO the unidentate specie suffers a steady transformation to the more stable bidentate specie before it disappears at 1033 K. This peculiar behavior is a central point to explain the catalytic synergy exhibited by the 10% CaO + 90% MgO mixture as compared to the pure components. Besides carbonates, several species are generated during the heating process, i.e., during CO_2 release and re-adsorption in the presence of adsorbed water and/or hydroxyl groups. These species, some of them intermediates of the reactions involved in naphthalene gasification, would correspond to formiate species, from the interaction of adsorbed CO with OH groups; carboxylic groups with hydrogen bond or aldehydic groups. These species showed a greater stability for pure CaO than for pure MgO and the mixture since they can be found up to 873 K in pure CaO, but only up to 723 K in pure MgO and the 10% CaO+90% MgO mixture.

Exposure to CO_2, as well as its adsorption at ambient temperature, generates carbonates, formiate, carboxylic acids with hydrogen bonds and aldehydic species, whose IR bands intensities varied in the following order: MgO, 10% CaO + 90% MgO and CaO. Carbonates in pure MgO and 10% CaO + 90% MgO are of the unidentate type, while in pure CaO are of the bidentate type. Exposure of pure MgO to $H_2O_{(V)}$, produces a fast disappearance of the species formed in the CO_2 adsorption. For 10% CaO + 90% MgO, the unidentate specie disappears more slowly to a prolonged exposure to $H_2O_{(V)}$. For pure CaO, the formed species are more stable since they remained after a long (30 min) exposure to $H_2O_{(V)}$. Further details of DRIFTS experiments are given in [5].

Table 3 shows the IR bands reported in the literature [7,9–13,15] for the carbonate and formiate species. Assignments are different as the solids originated from different precursors and they were subjected to different pretreatments. The carbonate species differ in the gap of the asymmetric tension band of the carbonate ion (ca. 1415 cm^{-1}), which are 100, 300, 400 cm^{-1} or more for the unidentate, bidentate and bridge carbonates, respectively. Other IR bands reported are shown in Table 4 [10,16–19].

3.3.3. XPS analysis

XPS results (Tables 5–7) showed a significant reduction (8.0–4.4 at.%) of the atomic percentage of the carbonates in pure MgO; while in pure CaO and in 10% CaO+90% MgO, this reduction was small (16.9–15.3 and 4.2–3.3 at.%, respectively). The 10% CaO + 90% MgO catalyst shows the smallest content of carbonates among the three solids assayed. Deposited char increases in all the solids during the reaction and the content of the carbonaceous matter in the deposited material showed the following order: 10% CaO + 90% MgO < pure MgO < pure CaO. The latter indicates that the mixture has a larger capacity to inhibit char deposition as compared to the pure oxides. The smaller amount of carbonates in 10% CaO + 90% MgO and in pure MgO confirms their smaller stability in these solids as compared with those formed in pure CaO. The atomic percentage of

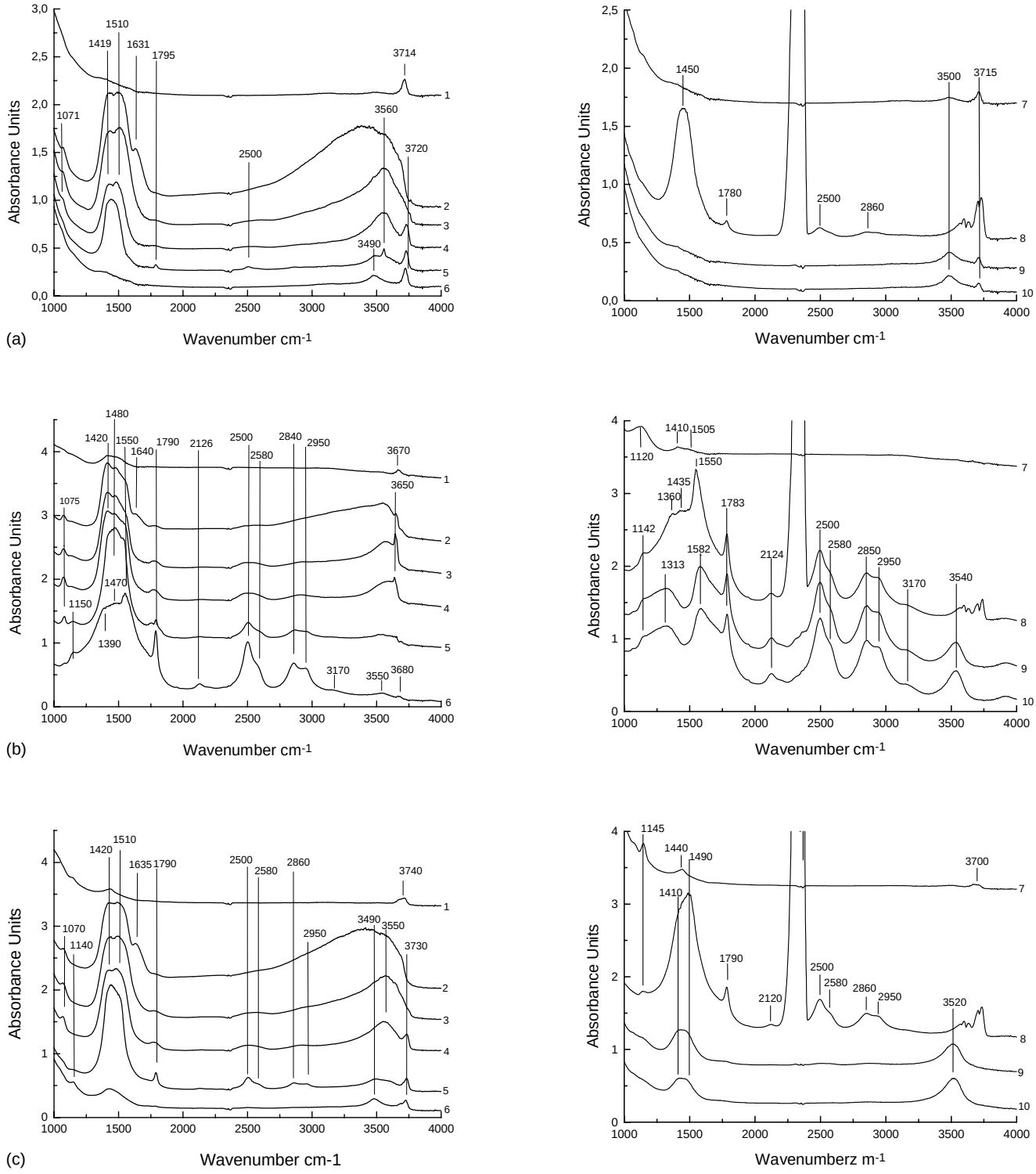

Fig. 7. DRIFT spectra after degasification at 1033 K, plus in situ CO_2 and H_2O treatment: (a) MgO; (b) CaO; and (c) 10% CaO + 90% MgO. Curves—1: after cleaning with N_2 at 1033 K for 1 h; 2: after CO_2 elimination and N_2 at RT for 10 min; 3: after heating to 423 K in N_2 for 30 min; 4: after heating to 573 K in N_2 for 30 min; 5: after heating to 723 K in N_2 for 30 min; 6: after heating to 873 K in N_2 for 30 min; 7: after heating to 1033 K in N_2 for 30 min; 8: after adsorption of CO_2 at 1033 K for 10 min; 9: after being subjected to $N_2 + H_2O$ at 1033 K for 5 min; 10: after being subjected to $N_2 + H_2O$ at 1033 K for 15 min.

Table 3
IR assignations for carbonates and formiate species

Unidentate (cm^{-1})	Bidentate (cm^{-1})	Bridge (cm^{-1})	Bicarbonate (cm^{-1})	Formiates (cm^{-1})	Literature
1530–1470	1630–1590	1660–1620			[10]
1370–1300	1270–1260	1410–1290			
1080–1040	1030–1020	1050–990			
880–850	840–830	840–830			
820–750	760–740	705–695			
690–670	680–660	1750			
1500	1635–1550	1275			
1420	1315–1290				[11]
1060	1050				
860	980–850				
1496	1642			2840; 1604; 1370	[12]
	1332				
1420–1410	1570–1560	1760–1720		2810; 1610; 1300	[13]
1350	1420	1780–1700			
	1350–1320				
				Three types of formiate—unidentate: 2811, 1649, 1304; bidentate: 2750–2715, 1610, 1388; bridge: 2839, 1622, 1342	[15]
1526–1461	1629–1619	1797–1776	1658–1630		[9]
1063–1075	1304–1299		1472–1415		
			1223–1213		
			ν_{OH} at 3610 cm^{-1}, 1230 cm^{-1}	High ν_{OH}, ν_{CO} at 2143 cm^{-1}	[7]

Table 4
IR assignations for adsorbed water, carboxylic groups and aldehydes

Specie	Wave number IR bands	Literature
Adsorbed water	Broad band at 3525 cm^{-1}	[10]
	Broad band between 3600 and 2800 cm^{-1}	[17]
	Broad band at 3600 and shoulder at 1640 cm^{-1}	[18,19]
Carboxylic acid	ν_{CO} at 1690–1760 cm^{-1} and ν_{OH} at 3500–3650 cm^{-1}	[16]
Carboxylic acid with H-bridge	ν_{CO} at 1690–1760 cm^{-1} and ν_{OH} at 2500–2700 cm^{-1}	[16]
Aldehydes	ν_{CO} at 1690–1760 cm^{-1} and ν_{CH} at 2900–3000 cm^{-1}	[16]

Table 5
XPS analysis of MgO

Element	Fresh		Used		Calcined, 1033 K, 30 min		H_2O-pretreated, 1033 K, 2 h	
	BE	at.%	BE	at.%	BE	at.%	BE	at.%
C 1s	284.8	10.2	284.8	19.4	284.8	12.9	284.8	9.4
C 1s	286.3	3.2	286.3	10.7	286.3	2.2	286.3	2.1
C 1s	289.8	8.0	289.8	4.4	289.8	3.0	289.5	1.7
O 1s			530.3	11.5	530.0	24.7	530.0	26.8
O 1s	531.6	51.0						
O 1s			532.4	20.1	532.0	15.8	531.8	18.2
Mg 2s	88.8	27.6	89.1	33.8	88.3	41.3	88.3	41.9
Ca 2s								
Ca/Mg								
Ca/C								
Mg/C		1.3		1.0		2.3		3.2
$C/CO_3^{=}$ [a]		2.7		7.8		6.0		7.7

[a] C: total carbon; $CO_3^{=}$: C 1s ~290 eV.

Table 6
XPS analysis of CaO

Element	Fresh		Used		Calcined, 1033 K, 30 min		H_2O-pretreated, 1033 K, 2 h	
	BE	at.%	BE	at.%	BE	at.%	BE	at.%
C 1s	284.8	17.7	284.8	26.3	284.8	19.3	284.8	22.0
C 1s	286.3	2.5	286.3	17.1	286.3	5.1	286.3	4.2
C 1s	289.4	16.9	290.5	15.3	289.6	15.6	289.6	15.3
O 1s								
O 1s	531.2	49.9			531.5	47.7	531.5	46.7
O 1s			532.4	32.7				
Mg 2s								
Ca 2s	438.5	13.0	439.7	8.6	438.7	12.4	438.8	11.8
Ca/Mg								
Ca/C		0.35		0.15		0.31		0.28
Mg/C								
$C/CO_3^{=}$ [a]		2.2		3.84		2.56		2.71

[a] C: total carbon; $CO_3^{=}$: C 1s ~290 eV

carbonates in pure MgO subjected to either calcination or to $H_2O_{(V)}$ treatment follows the same behavior as the used solid, i.e., decreases as compared to the fresh catalyst. Again, this reflects the carbonates instability on MgO at the reaction temperature and in the presence of $H_2O_{(V)}$. Calcination and H_2O treatments do not produce a carbonate reduction in the mixture as compared to the fresh mixture, but for all conditions, the carbonate content is significantly smaller that carbonate contents in pure CaO. In this regard, the mixture behavior is similar to pure MgO.

Formation of a new species containing oxygen during the reaction was detected for both pure MgO and the mixtures, as shown by a new O 1s peak at 530 eV, associated to an O^{2-} form, which corresponds to oxygen bounded to the metal M–O (see O 1s's peak assignations for different oxygen species in reference [5]). The generation of these species is attributed to the removal of OH and/or carbonate groups during the reaction, which is confirmed by the reduction of the O 1s atomic percentage and of carbonate in these solids during the reaction. These solids exhibit the same behavior when subjected to calcination and steam treatment at the reaction temperature, indicating the O^{2-} presence. A different behavior is observed with pure CaO, calcined CaO or CaO treated with $H_2O_{(V)}$ at the reaction temperature, as no new species were formed.

Even though char deposition does occur during the reaction, the Ca/C ratio is approximately constant for the fresh and used 10% CaO + 90% MgO mixture (0.03–0.04 at.%), whereas in pure CaO this ratio decreases from 0.35 to 0.15 at.%. This suggests that Ca in the mixture behave differently than in pure CaO, i.e., Ca behaves different in contact with Mg with respect to the carbonate formation and the char deposition; this result, suggests strongly that Mg might inhibit carbonaceous material deposition and carbonate formation.

The Mg 2s atomic percentage in the mixture as compared to pure MgO remains constant during the reaction (32.7 and 32.8 at.%), suggesting that atom transfer between oxides

Table 7
XPS analysis of 10% MgO + 90% MgO

Element	Fresh		Used		Calcined, 1033 K, 30 min		H_2O-pretreated, 1033 K, 2 h	
	BE	at.%	BE	at.%	BE	at.%	BE	at.%
C 1s	284.8	9.1	284.8	18.6	284.8	13.6	284.8	16.7
C 1s	286.3	2.6	286.3	7.7	286.3	2.3	286.3	3.4
C 1s	289.5	4.2	290.2	3.3	289.6	4.5	289.6	5.7
O 1s			530.1	5.6	529.8	20.4	530.4	22.6
O 1s	531.2	51.0						
O 1s			532.0	30.9	531.8	19.8	532.2	16.9
Mg 2s	88.4	32.7	89.0	32.8	88.4	38.4	88.6	32.6
Ca 2s	438.9	0.5	439.5	1.2	438.5	1.2	438.7	2.1
Ca/Mg		0.02		0.04		0.03		0.06
Ca/C		0.03		0.04		0.06		0.08
Mg/C		2.0						
$C/CO_3^{=}$ [a]		3.8		9.00		4.55		4.54

[a] C: total carbon; $CO_3^{=}$: C 1s ~290 eV.

does not occur or it is minimal; this would indicate that the synergetic effect may not be explained by surface contamination. On the contrary, Ca 2s in the 10% CaO + 90% MgO mixture increases its atomic percentage from 0.5 to 1.2 at.% for pure CaO, indicating that a fraction of the CaO in the mixture is free of carbonates and carbonaceous material. Further details of XPS experiments are given in [5].

4. Discussion

4.1. Synergy between CaO and MgO

Catalytic synergy was observed in practically all the range of mixtures assayed (CaO content larger than 5%), i.e., carbon conversion during naphthalene gasification with CaO + MgO mixtures is larger than the pure oxides contribution. The largest synergy, with a value of 44.2%, was observed with the 10% CaO–90% MgO mixture (carbon conversion $X_C = 79\%$). Pure MgO and CaO showed carbon conversions of 54 and 62%, respectively. Previous works of García and Hüttinger [1,2] about the homogeneous gasification of naphthalene showed, at all temperatures, very low yields of hydrogen, methane, carbon monoxide and carbon dioxide, with maximum naphthalene conversions lower than 0.05. The main products formed in that case were solid deposited carbon and tar. From these results, one may assume a negligible contribution of the non-catalyzed homogeneous reaction to the conversion values obtained during the catalytic gasification.

As shown by XRD analysis, the lack of formation of new phases and the absence of any kind of mutual chemical contamination between MgO and CaO in the mixture strongly suggests that oxides in mixture behaves as if they were unmixed. The same conclusion can be withdrawn from BET analysis of surfaces where the values for the mixtures correspond to the value of the weighted area of the pure components. An important fact is that the Mg 2s XPS atomic ratio percentage in the mixture remains constant during the reaction, strongly suggesting that contamination by surface atoms transfer between the oxides seems to be excluded. On the other hand, the binding energy corresponding to Ca 2s and Mg 2s peaks remains unchanged during the reaction, which could support the fact that oxides have not been modified or that no new phase associating Mg with Ca has been formed. Therefore, it could be accepted that during the catalytic reaction, oxides remain unchanged and that the synergetic effect could be explained as a catalytic cooperation between both oxides that keep a good contact. On the other hand, from the XRD, DRIFT and DTG/DTA analyses, it can also be concluded that MgO exhibits a lesser carbonation capacity than CaO.

The catalytic behavior of the mixture resembles more to that of MgO than that of CaO, suggesting, in CaO and in the 10% CaO-containing mixture the existence of sites of different nature than in MgO.

4.2. Effect of the residence time in the formation of reaction products

Carbon conversion increases with the residence time (τ) in the reactor. While the increase for $\tau < 2$ s is due to CO, CO_2 and CH_4 contribution, for values of $\tau > 2$ s the CO_2 yield becomes constant, thus the observed carbon conversion increase results only from an increase of the CO and CH_4 yields that grow slower than for the case with $\tau < 2$ s. According to the mechanism proposed in a previous study [1], the first stage of the reaction corresponds to the irreversible dissociation of the naphthalene molecule on the vacant active sites of the catalyst's surface, generating hydrogen, methane and deposited solid carbon as seemingly primary products, as probably more than one step is needed to generate hydrogen and methane. The solid carbon reacts with steam, in a second step, to produce carbon monoxide and/or carbon dioxide.

The yield curves obtained in this work may be explained in terms of this mechanistic pathway. At low residence times ($\tau < 2$ s), product formation is small because of an insufficient contact time between naphthalene and the catalyst in the reaction bed. Thus, hydrogen and solid carbon yields are small and, therefore, CO and CO_2 yields are small as well. As the residence time increases, a higher contact time between the reactant and the catalyst favors the dissociation of the naphthalene molecule, with solid carbon formation on the surface of the catalysts. As a result of reactions between this solid carbon deposited with steam and CO, higher gaseous yields are obtained. Finally, at the highest assayed residence times, carbon deposited and carbonate formation increase significantly, deactivating part of the catalyst's sites that leads to a measured stabilization in the yield of the gaseous products.

With regard to the CO and CO_2 yields', it can be stated that, because of the higher availability of free catalyst's sites, at low residence times, and as a consequence a favored occurrence of the shift reaction, CO_2 formation is more important than CO. However, at higher residence times, the shift reaction is affected by a lesser availability of sites, the latter being deactivated by deposited carbon and carbonate formation, and CO formation becomes more important than CO_2. This assumes that shift reaction sites are the same active sites than those for carbon oxidation and naphthalene dissociation.

4.3. Consequences of the cooperation between CaO and MgO

Differences in carbonate formation would reflect the differences between basic sites in MgO and CaO. It is well known [8,9,12] that, according to their type, carbonates exhibit a different behavior during the reaction. When unidentate carbonates are formed, adsorption takes place through a carbon atom bond of the CO_2 molecule with an oxygen atom from the catalyst releasing a metallic atom. When bidentate

carbonate is formed adsorption proceeds through a carbon atom bond of the CO_2 molecule with basic oxygen from the solid and the simultaneous binding of oxygen from the CO_2 to the metallic atom of the catalyst [14].

The greater stability of the bidentate carbonate formed in the pure CaO surface could deactivate its sites and, hence, inhibit adsorption and the dissociation of steam affecting the necessary step for char gasification and for the occurrence of the "shift" reaction involved in the gasification mechanism [1,2,15]. This would not be the case for the catalytic effect of pure MgO or for the mixture where the free cation exposure to steam favors its adsorption and the subsequent formation of hydroxyl groups in sufficient amounts so that gasification can proceed.

The effect of MgO in cleaning the surface and freeing basic sites occupied by carbonates and deposited carbonaceous material in CaO evidences cooperation in the 10% CaO + 90% MgO mixture. As stated in a previous section, and observed in curve 7 of Fig. 7, MgO and the 10% MgO-containing catalysts show OH groups at the reaction temperature of 1033 K, while the CaO catalyst does not. This is the basis to explain the cooperative effect of MgO with respect to the CaO catalyst. Furthermore, when CO_2 is introduced (curve 8 of Fig. 7) carbonates, formiate, carboxylic acids and aldehydic species are formed [5] whose characteristic IR bands are shown in Table 3. Again, differences between the bands for the CaO catalyst for one part, and the bands for the MgO and MgO-containing mixture are evident. In fact, carbonates are of a bidentate nature for the former, and of a unidentate nature, for the latter. When steam is introduced (curves 9 and 10), nearly all of the carbonaceous matter disappears from the pure MgO and MgO-containing mixture, but they remain in the CaO catalyst. These observations suggests strongly that when exposed to an expected ambient of CO_2/H_2O, the CaO catalyst will keep highly stable bidentate carbonates, thus blocking active sites, while mixtures with MgO will generate less stable unidentate carbonates thus allowing a cleaner surface for further reaction. Thus, the fast decomposition of unidentate carbonate at the reaction conditions contributes to the formation of intermediate compounds, such as formiate, carboxylic and aldehydic groups. The reaction with steam easily removes these compounds, particularly the formiate.

The same cleaning effect produced by MgO over the CaO in the mixture is shown by the DTG/DTA results, thus confirming the cooperative effect described above. This is made evident by a lower combustion temperature of deposited char when a mixture is utilized than for the pure components. This temperature decrease could be explained by the inhibition of stable carbonate formation on the CaO surface. This inhibition would be promoted by the MgO presence, thus generating greater activity of CaO in the char combustion, characterized by a lower temperature.

These results give rise to some speculations: a migration of OH^- cannot be excluded. As discussed above, the OH species could participate in the reaction mechanism. Obviously, the OH at the interface of both oxides could play this role. But the OH species formed on MgO might also migrate towards the CaO surface through a "spillover" process; these species might react in the CaO surface reacting or generating sites that would allow the formation of unidentate carbonate and, consequently, diminishing the bidentate carbonate formation, as discussed above. At this state of the discussion, we could also make additional speculations. Other species could be also present and be able to migrate. H species migration cannot be ruled out; in this case, the atomic hydrogen would react with char precursors inhibiting its formation. Similar comments could be made with oxygen species and spillover processes. Phenomena of this kind, in particular reaction of hydrogen and oxygen spillover with carbon precursors, have been previously reported in the literature through isotope interchange for the H, OH and O species during several reactions involving metals, oxides, alumina, zeolites, etc. [20–22]. Although this phenomenon might be involved in the mixtures, this explanation at this moment is just a speculation and needs further experimental work.

5. Conclusions

Mixtures of CaO + MgO with 5% or more of CaO exhibit catalytic synergy in naphthalene gasification. The 10% CaO + 90% MgO mixture exhibited the greatest synergy (44%). Carbon conversion of the mixture (79%) was larger than the ones exhibited by the pure oxides (54 and 62% for MgO and CaO, respectively).

Characterization of the mixture exhibiting the greatest synergy and of the pure components through SBET, DRX, TGA, DTG/DTA, XPS and DRIFT (in situ) techniques does not allow an explanation for the observed synergy from the formation, during the reaction, of a phase different from the phases presented by the fresh solids. No correlations were found between the catalytic activity and the catalysts SBET or with basicity measured by CO_2 adsorption (TGA) and $CDCl_3$ (DRIFTS).

DRIFTS and XPS analyses did not show correlation between basicity and the catalytic activity; however, carbonate formation and char deposition on the catalysts' surface was observed. Moreover, formiate, carboxylic and aldehydic species were formed during simulation of the reactive atmosphere of gasification. XPS analysis did not give a clue of the existence of some phenomenon of contamination between the metallic components forming the oxides during the catalytic reaction.

For the catalysts MgO and 10% CaO + 90% MgO the formed carbonates in the surface are of the unidentate type and unstable in the presence of $H_2O_{(V)}$. In pure CaO the carbonates are of the bidentate type and quite stable, even in the presence of $H_2O_{(V)}$.

The synergetic effect of the 10% CaO + 90% MgO mixture on naphthalene gasification might be explained by a catalytic cooperation, as separated phases, between the Mg

and Ca oxides, acting on its own. MgO would be responsible for the inhibition in the formation of bidentate carbonate and carbonaceous material deposition on the CaO surface, thus promoting the formation of the less stable unidentate carbonate in CaO. It cannot be excluded the role-played by species spillover processes.

Acknowledgements

The support of FONDECYT-Chile, -Grant 1980474 and a fellowship granted by the Andes Foundation to one of the authors (NA), are gratefully acknowledged. The authors acknowledge the "Fonds National de la Recherche Scientifique (FNRS)" of Belgium for their financial support for the acquisition of the XPS and XRD equipments.

References

[1] X.A. García, Gasificación no-Catalítica y gasificación catalítica de naftaleno con vapor de agua, Tesis doctoral, Universidad de Concepción, Chile, 1991.
[2] X.A. García, K.J. Hüttinger, Erdöl und Kohle-Erdgas-Petrochemie 43 (7–8) (1990) 273.
[3] G.E. Betancur, A.L. Gordon, X.A. García, in: J.A. Pajares, J.M.D. Tascón (Eds.), Coal Science and Technology, vol. 24, Elsevier, Amsterdam, The Netherlands, 1995, p. 707.
[4] X.A. García, N.A. Alarcón, A.L. Gordon, Fuel Process. Technol. 58 (1999) 83.
[5] N. Alarcón, X. García, M.A. Centeno, P. Ruiz, A. Gordon, Surf. Interf. Anal. 31 (2001) 1031.
[6] Mineral Powder Diffraction File, Data Book, JCPDS, International Centre for Diffraction Data, Park Lane, Swarthmore, PA, 1986.
[7] J.C. Lavalley, Catal. Today 27 (1996) 377.
[8] E.A. Paukshtis, N.S. Kotsarenko, L.G. Karakchiev, React. Kinet. Catal. Lett. 12 (1979) 315.
[9] R. Philipp, A. Omata, A. Aoki, K. Fujimoto, J. Catal. 134 (1992) 422.
[10] J.V. Evans, T.L. Whateley, J. Chem. Soc., Faraday Trans. 63 (1967) 2769.
[11] Y. Fukuda, K. Tanabe, Bull. Chem. Soc. Jpn. 46 (1973) 1616.
[12] G.W. Wang, H. Hattori, J. Chem. Soc., Faraday Trans. I 80 (1984) 1039.
[13] F. Solymosi, H. Knözinger, J. Catal. 122 (1990) 166.
[14] K. Tanabe, M. Misono, Y. Ono, H. Hattori, in: Delmon, J.T. Yates (Eds.), Studies in Surface Science and Catalysis, vol. 51, Elsevier, Amsterdam, 1989, p. 17.
[15] T. Shido, K. Asakura, Y. Iwasawa, J. Catal. 122 (1990) 55.
[16] D.A. Skoog, J.J. Leary, Principles of Instrumental Analysis, McGraw-Hill, Madrid, 1994.
[17] G.C. Maiti, M. Baerns, Appl. Catal. A 127 (1995) 219.
[18] J.J. Benitez, A. Diaz, Y. Laurent, J.A. Odriozola, Catal. Lett. 54 (1998) 159.
[19] M.A. Centeno, M. Debois, P. Granje, J. Phys. Chem. B 102 (35) (1998) 6835.
[20] P. Ruiz, Y.W. Li, E. Gaigneaux, B. Delmon, in: Proceedings of the International Symposium on the Dynamics of Surface and Reaction Kinetics in Heterogeneous Catalysis, Antwerp, Belgium, September 15–17, 1997.
[21] K.-D. Jung, T. Bell Alexis, J. Catal. 193 (2) (2000) 207.
[22] T. Maillet, Y. Madier, R. Taha, J. Barbier Jr., D. Duprez, Stud. Surf. Sci. Catal. 112 (1997) 267.